

ALBEDO CHANGES ON MARS: THE ROLE OF DUST AEROSOLS AS SEEN BY OMEGA. Mathieu Vincendon¹, Y. Langevin¹, F. Poulet¹, A. Pommerol², M. J. Wolff³, J-P. Bibring¹, B. Gondet¹, D. Jouglet¹, and the OMEGA team,¹Institut d’Astrophysique Spatiale, CNRS/Université Paris Sud, Orsay, France (mathieu.vincendon@ias.u-psud.fr),²Laboratoire de Planétologie de Grenoble, UJF/CNRS, Bât. D de Physique, B.P. 53, 38041 Grenoble Cedex 9, France,³Space Science Institute, 18970 Cavendish Road, Brookfield, WI 53045, USA.

Introduction: The apparent reflectance of dark surfaces changes with time. These variations are due to change in the aerosols loading, change in the viewing or lighting conditions, or deposition and removal of dust at the surface ([1], [2], [3]). We analyze here time series of OMEGA near-IR observations of low albedo regions of Mars using a radiative transfer code [4] to disentangle these different possibilities. Albedo variations are found to be primarily due to aerosols during the [2004-2008] period, with no widespread surface variations seen in the middle of the analyzed dark regions.

Time series: We constituted 11 time series of reflectance spectra of 11 different dark regions located between 40°S and 40°N. Reflectance spectra are obtained by OMEGA with different lighting and viewing conditions. Strong variations are observed in both the level of reflectance and the shape of the near-IR spectrum (see Figure 1).

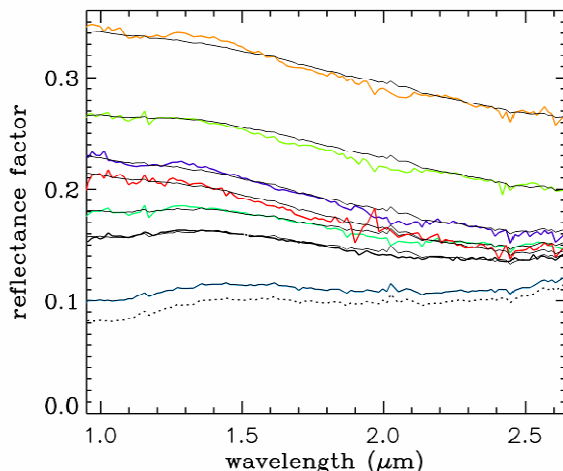


Figure 1: Time series of OMEGA observations at 306.5°E, 25.5°S (Mare Erythraeum). Observations are in colors, and model fit in thin solid line. The dotted line is the surface spectrum estimated from the blue observation. See Table 1 for details. Data are calibrated as “reflectance factor”, i.e. $I/F/\cos(i)$.

We have modeled these time series using the assumption that all variations are due to aerosols. We use the radiative transfer code and the optical parameters described in [4]. Surface properties (Lambert assumption) are estimated from observations

obtained with low aerosol optical depths according to [5]. We have looked for the optical depth at 0.9 μm and the spectral dependence of the optical depth that provide the best fit of each observed spectra obtained at higher dust loading. Results for the example of Figure 1 are indicated on Table 1. The evolution of the spectral properties with time can be well modeled through variations in the optical thickness of aerosols and the assumption of an unchanging surface reflectance.

Table 1: Parameters of the observations shown in Figure 1. L_S : solar longitude; MY: Martian Year; i : solar zenith angle; e : emergence angle; φ : phase angle. The results of each model fit are indicated: τ , the optical depth at 0.9 μm and S , the “slope factor” (i.e. the ratio of optical depth $1\mu\text{m}/2.5\mu\text{m}$).

Color	L_S (°)	MY	i (°)	e (°)	φ (°)	τ	S
black	348	26	24	0	25	1,3	1,7
purple	243	27	75	1	75	1,0	2,9
blue	94	28	55	2	54	0,3	1,8
cyan	215	28	61	9	51	1,0	1,8
green	277	28	6	8	14	2,9	1,6
yellow	307	28	25	75	90	1,6	2,1
red	3	29	80	0	80	0,8	4,5

Comparison with the MERs: The PanCam instruments onboard both Opportunity and Spirit estimate each day the optical depth of aerosols from the ground via direct solar extinction measurements. Optical depth retrievals have been available since the beginning of the Mars Express mission ([5], and personal communication). This makes it possible to compare values derived from the OMEGA dataset to the ground truth obtained by the MERs. Results are presented in Figure 2: the variations of the observed surface spectrum from orbit lead to modeled optical depths that are fully consistent with that measured from the ground by the MERs. Observed albedo variations from orbit therefore result primarily from change in the contribution of aerosols.

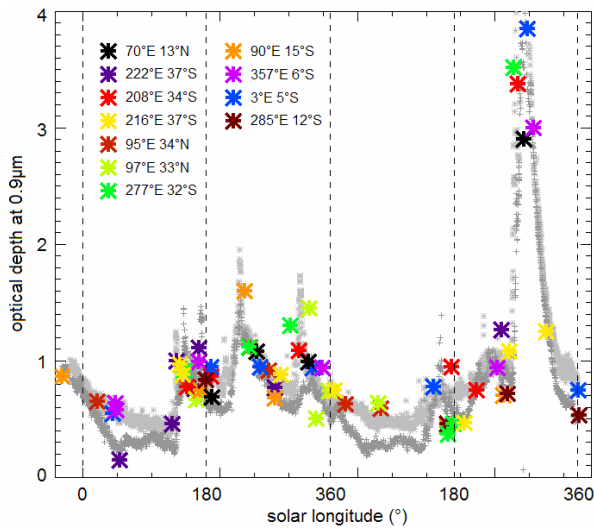


Figure 2: Optical depths at 0.9 μm as a function of time, from early 2004 to early 2008. Color stars: model results for OMEGA observations of dark terrains situated at mid-latitudes (40°S-40°N). Dark grey crosses: PanCam/Spirit measurements [5]; Light grey stars: PanCam/Opportunity measurements [5].

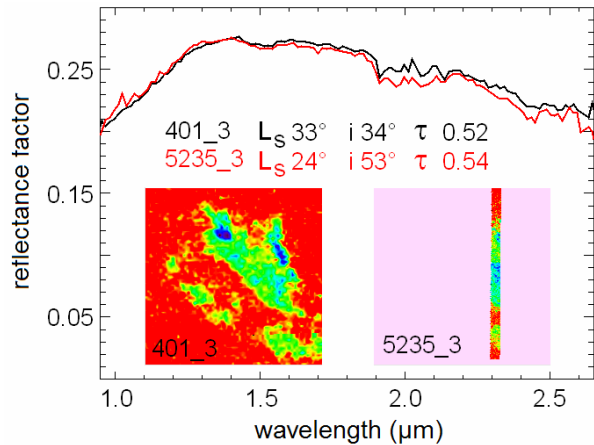


Figure 3: Comparison between two observations of Aram Chaos obtained in early 2004 (# 401_3) and early 2008 (#5235_3). Spectra of the region at 339.9°E, 3.3°N and hydration map (1.9 μm band depth, from red – no hydration – to dark blue) are shown. The contribution of dust aerosols is weak and similar for both observations (optical depths measured by the MER [5] and solar incidence angles are indicated). Surface properties are similar before and after the 2007 planet-encircling dust storm.

Surface deposits: This result indicates that no significant surface deposits that persist several weeks are required to explain albedo change of dark regions. This is notably true after the 2007 planet-encircling dust storm. When seen through similar atmospheric

conditions, surface spectra are similar before and after the dust storm, within a few % (Figure 3). Significant albedo increases are expected from the fallout of the large amount of dust observed in the atmosphere during dust storms (see e.g. measurements above the PanCam calibration target, [6]). They are not observed at the center of dark regions. Such increases are on the other hand sometimes observed near the boundaries between bright and dark regions, in agreement with recent studies [2].

Variations of the size of dust aerosols: We have demonstrated that the apparent variations of the reflectance of dark regions are due to aerosols. We observe that the decreasing spectral slope that characterizes the contribution of aerosols varies with time (Figure 1 and Table 1). We have converted this spectral slope to an effective radius of aerosols using a T-Matrix code [7]. The resulting mean particle size of aerosols varies between less than 1 μm and 2 μm . For instance, it decreases during the decay of the 2007 planet-encircling event (Figure 4). A similar behavior have been previously observed by [8] and is generally explained by the faster settling of the large particles raised during the storm compared to small particles.

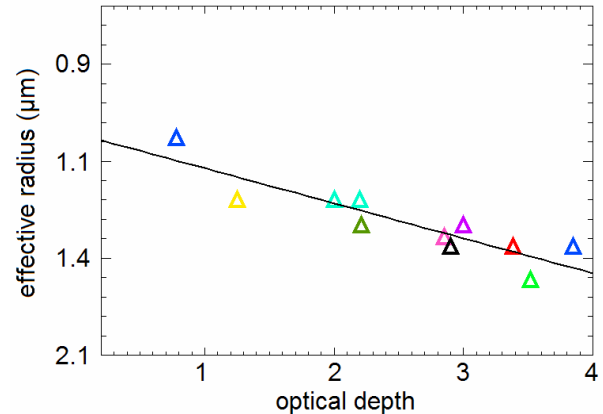


Figure 4: Variations of the effective radius of the aerosols layer during and after the planet-encircling dust event of 2007 ($L_s > 265^\circ$, MY28).

References: [1] Sagan, C, et al. (1972), Icarus 17, 346-372. [2] Geissler, P. E. (2005), JGR, 110, E02001. [3] Szwast, M. A., et al. (2006) JGR, 111, E11008. [4] Vincendon, M., et al. (2007), JGR, 112, E08S13. [5] Lemmon, M. T., et al. (2004), Science, 306, 1753– 1756. [6] Kinch, K. M. et al. (2007) , J. Geophys. Res., 112, E06S03. [7] Mishchenko, M. I., L. D. Travis (1998), J. Quant. Spectrosc. Radiat. Transfer, 60, 309-324. [8] Wolff, M. J., T. Clancy (2003), J. Geophys. Res., 108, E9, 1-1, 5097.